Chaos, Solitons and Fractals 185 (2024) 114997

Contents lists available at ScienceDirect

Chaos, Solitons and Fractals

journal homepage: www.elsevier.com/locate/chaos

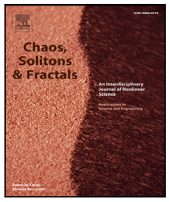

Two-dimensional cellular automata—Deterministic models of growth

Paolo Lazzari [a,*], Nicola Seriani [b]

[a] National Institute of Oceanography and Applied Geophysics - OGS, via Beirut 2, Trieste, I-34014, Italy
[b] The Abdus Salam ICTP, Condensed Matter and Statistical Physics Section, Strada Costiera 11, Trieste, I-34151, Italy

ARTICLE INFO

Keywords:
Cellular automata
Scaling
Surface growth
Family-Vicsek
Universality classes

ABSTRACT

Cellular automata are simple discrete deterministic rules that can however produce different, from simple to very complex, dynamics, and it would be useful to have a criterion to classify their behaviour. Here, we argue that the investigation of surface growth as described by the cellular automata provides a quantitative method to classify them. To this aim, the growth behaviour of cellular automata describing pure growth has been analysed. The automata fall into three classes: a first class is formed by the rules where the surface width saturates, and includes also rules that display Family-Vicsek scaling. A second class is constituted by the rules where the surface width grows indefinitely, which we call the dendritic-growth class. Finally, some rules belong to the non-growing class. A quantitative analysis shows a finer sub-division in clusters, some of which are close to known models of growth, while others do not have any counterpart in the literature. This work demonstrates the capabilities of deterministic cellular automata to describe a large variety of growth regimes, and suggests that their growth behaviour may be also used as an effective tool for their classification.

1. Introduction

Cellular automata (CA) are discrete deterministic algorithms that, using simple rules, are able to produce a variety of different behaviours, from periodic to chaotic. It would therefore interesting to be able to classify them according to their behaviour, also because cellular automata are ubiquitous in science and technology. The basic idea was developed by von Neumann [1], and it is attractive for its ability to simulate systems of interacting entities with simple rules, which may however generate complex and unpredictable behaviour. Some of them, such as Conway's Game of Life [2], were used as models of biological processes. More recently, cellular automata have been shown to quantitatively reproduce pattern growth in real systems, such as lizard skin [3,4], mussel beds [5], and tumours [6]. It was demonstrated that specific CA have the capability of reproducing complex behaviours implementing a Universal Turing machine [7]. Finally, a cellular automaton is used in the scientific package Mathematica to generate pseudo-random numbers. Despite their seeming simplicity, they are known to display a large variety of behaviours, from periodic to chaotic.

Cellular automata display a wide variety of behaviours, and for this reason, it is desirable to find a way to classify them according to these differences. Surprisingly, a complete classification of cellular automata has been accomplished only for the case where the space is one dimensional (1D). Wolfram classified the 1D CA in four classes, depending on their long-time behaviour [8]. Such classification does not exist in higher dimensions. Moreover, we note that this classification is very qualitative, distinguishing only whether the initial patterns evolve into (1) stable, homogeneous patterns; (2) oscillating patterns; (3) pseudo-random or chaotic patterns; and (4) complex patterns. Classification is therefore one of the main open problems in the study of cellular automata [9]. A more quantitative approach used the roughness exponent of the spatio-temporal configurations of 1D CAs, but only managed to distinguish the class (4) from the others [10].

Here we address the problem of investigating and classifying the behaviour of a set of 2D CA (pure-growth cellular automata), and we argue that a more quantitative classification can be obtained, based on the growth behaviour of starting configurations with randomly filled sites on the lattice. This combines the various behaviours of deterministic rules with the random fluctuations in the initial conditions. This situation mimics growth processes in physics, chemistry and biology, and allows to put CA in the broader context of models of growth that have played a great role in the last decades.

Moreover, this approach is relevant also for the study of growth processes. Growth processes are ubiquitous in nature, and regard systems as diverse as surfaces and interfaces in materials [11,12], nanoparticles [13], colonies in ecology, bones and tissues in biology [3], and water droplets in atmospheric science. Different growth mechanisms can lead to different morphologies of the involved entities, and this affects their interaction with the environment in a crucial way: in materials, rough surfaces result in increased friction and enhanced chemical

* Corresponding author.
E-mail address: plazzari@ogs.it (P. Lazzari).

https://doi.org/10.1016/j.chaos.2024.114997
Received 9 February 2024; Received in revised form 4 April 2024; Accepted 10 May 2024
Available online 28 May 2024

reactivity; malignant tumours have more often irregular shapes than benign tumours. Correspondingly great is the interest in understanding and controlling these growth processes. Several models have been developed that are able to reproduce growth processes in a universal fashion, but limited to certain regimes. Interestingly, models that differ in their microscopic mechanisms may lead to the same long-time and long-distance behaviour, as described by the critical exponents of time and length dependence. They belong then to the same universality class. Only a few universality classes are known. Among models of growth, the Kardar-Parisi-Zhang [14] and the Edwards-Wilkinson [15] models belong to different universality classes, and physically correspond to different limiting regimes of growth. In cases of correlated noise, one can have a whole continuum of critical exponents, as in Ref. [16], where they were able to have the roughness exponent α continuously changing from 0.5 to 1, and the growth exponent β from 1/3 to 1. It is rare and difficult to produce a model with an entirely different long-time and long-distance behaviour by modification of the known models. Here we show that a particular class of deterministic and discrete algorithms, known as cellular automata, contains members that cover a broad range of critical exponents, and therefore represent entirely different universality classes from one another, and from the known ones. This is intriguing because it provides a whole new playground for the description of growth processes and, moreover, it does so with a family of deterministic algorithms. Summarizing, we study the growth behaviour of a family of cellular automata, and in doing so we both provide a classification of cellular automata, and we show the power of cellular automata for the description of different regimes of growth.

More in detail, we have investigated a family of 2D cellular automata on a square lattice, and analysed the growth of surfaces from an initial random seed. This provides a classification scheme of the rules in term of their growth behaviour, namely in three classes, which we call the saturating class, the dendritic-growth class, and the non-growing class. Several automata belong to the first class and display a saturation of the surface width. Some of these also follow the Family-Vicsek scaling [17], which in itself is an unexpected finding. However, we also identified a behaviour where the surface width is unbound, and grows indefinitely. This behaviour mimics dendritic growth, and therefore we call this the dendritic-growth class. For some rules, the surface does not grow at all (non-growing class). Moreover, analysis of roughness exponent and growth exponent shows that each of the first two classes has a further sub-division in clearly separated clusters, thus providing a fine structure to the classification. These results suggest that the classification of cellular automata according to their growth behaviour is quantitative, robust, and useful. We propose that this classification scheme could be applied more generally to cellular automata. Finally, these findings demonstrate that cellular automata provide a unified framework for the investigation of a wide variety of growth regimes.

2. Methods

A (1+1) model of growth has been considered, on a two dimensional square lattice with Moore neighbourhood. Each site on the lattice has two possible states, as it can be empty or full (occupied). The Moore neighbourhood includes the 8 neighbouring sites in the square lattice. With this neighbourhood, the number of occupied sites in the neighbourhood ranges from 0 to 8, Fig. 1a . A useful way to represent these CAs is then shown in Fig. 1b, for the case of rule 5: an empty cell becomes full if and only if it has either 1 or 3 full neighbouring cells. The CA itself is indicated by a number deduced from the rule, using powers of 2: since in this rule the cell becomes full only with 1 or 3 neighbours, it is indicated as rule 5: $2^{1-1} + 2^{3-1} = 1 + 4 = 5$. This is analogous to Wolfram's nomenclature [8], and it is unambiguous.

The system is in (1+1) dimensions, in the sense that the surface is extended in one direction, and grows in the perpendicular direction [18–20]. The initial configuration consists in a flat surface

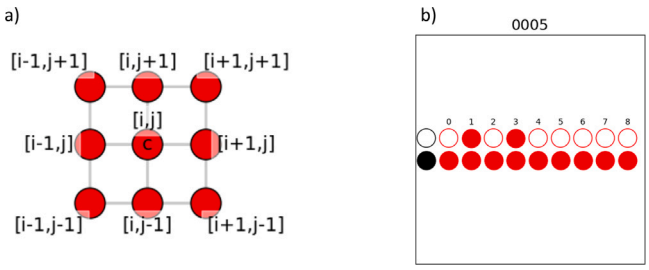

Fig. 1. (a) Schematic view of a Moore neighbourhood on a square two-dimensional lattice surrounding site 'c'. The Moore neighbourhood used in this study includes the central site 'c' and 8 surrounding sites. (b) Schematic view of the rule 5. The scheme indicates how the rule operates when the site 'c' is empty (first row) and when it is full (second row). In the shown case the red filled circles indicate that the empty cell gets filled when the number of occupied neighbours is equal to 1 and 3. Full sites always remain full, as shown in the second row, because we consider pure-growth rules. (For interpretation of the references to colour in this figure legend, the reader is referred to the web version of this article.)

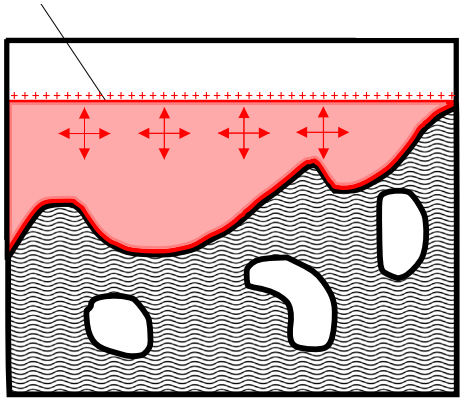

Fig. 2. Schematic view of surface identification in a 1+1 growth model. The wavy black area represents the state of full (occupied) sites at time t for the CA. At any given time the state of CA another cellular automaton (DCA) is initialized on a opposite row denoted by red plus symbols and propagates in all directions (red arrows) until it is stopped by the surface of CA state. The surface (red solid line) can therefore be determined by DCA. (For interpretation of the references to colour in this figure legend, the reader is referred to the web version of this article.)

perturbed by a random set of points. The initial seed consists of a first full layer and a second layer where each site is full with probability 0.5. Starting from these initial configurations, the state of the system was evolved deterministically with outer-totalistic pure-growth rules. The outer-totalistic rules are those whose dynamics depends only on the occupation of the central site and the number of occupied sites in the neighbourhood, i.e. in the 8 adjacent sites (Moore neighbourhood). The pure-growth rules are the rules that do not allow a filled site to become empty during the dynamics. In a 2D square lattice there are 256 such rules, and they have all been considered here. Clearly, the total number of rules on a square lattice with a Moore neighbourhood are many more, exactly $2^{2^9} = 2^{512} \sim 10^{154}$. They are not only too many to be studied computationally, but, also, most of them represent cases with no symmetry, which are physically difficult to justify. For this reason, we have chosen to limit this work to the full class of outer-totalistic pure-growth rules. A diagnostic cellular automaton (DCA), is used to find the surface. In short, the DCA is initialized in a non-occupied area above the surface of the CA state at a given time and it propagates in all the directions until it is blocked by the occupied sites of the CA state, Fig. 2. This allows to label the sites of the CA as surface sites. Notice that this definition allows for overhangs, at difference from solid-on-solid models.

In Fig. 3 rule 4 and 36 are shown. In rule 4 an empty site is filled at the next iteration when only 3 surrounding sites are occupied

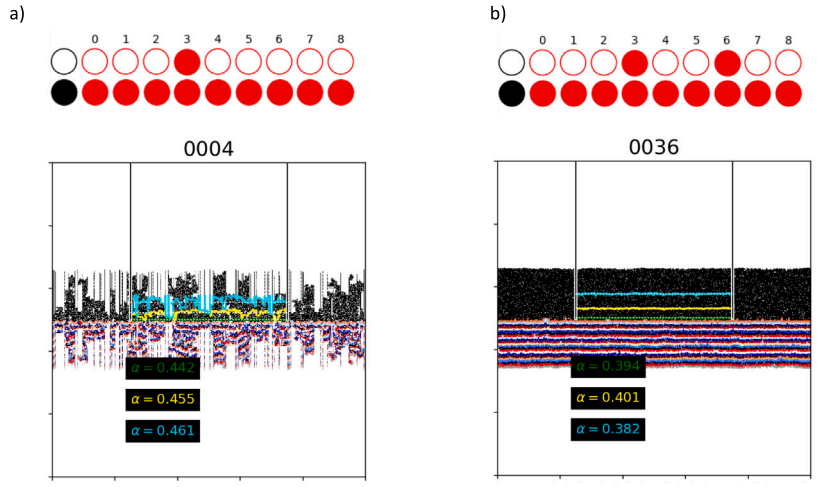

Fig. 3. Examples of single realizations of CA evolution for the rule 4 in cluster 3, of the dendritic-growth class (a), and rule 36 in cluster 2, of the saturating class (b). The top diagrams schematizes the rules. In case of void site (upper row indicated by empty black circle on the left) the site is filled in the next iteration if any 3 over 8 surrounding sites are already filled (rule 4) and for rule 36 the central site is filled if 3 or 6 surrounding sites are filled at previous step. The diagrams indicate also that if the site is filled (second row marked with filled black circle) for any occupation of the surrounding the site remains filled. To avoid interactions with the boundary conditions the statistics are computed only in the central region (L = 2500) limited by the vertical horizontal lines shown in both panels. The horizontal coloured lines represents the surface computed after 50 iteration (green), 500 iterations (yellow) and 1250 iterations (cyan). The corresponding roughness exponent α is reported. Upper and lower plots are symmetric with respect to x-axis; the surface is shown in the lower part at several numbers of evolution steps, with different colours to distinguish them. (For interpretation of the references to colour in this figure legend, the reader is referred to the web version of this article.)

(occupation level 3). In rule 36 an empty site is filled at the next iteration when 3 or 6 surrounding sites are occupied (occupation level 3 or 6). The evolution of the model state, according to the specific rule, is done iterating the application of the rule in each site of the domain simultaneously, therefore the time step is discrete. The simulations were performed using an open source Fortran-90 code. The model internally computes state and surface evolution. The domain is composed of 5000 × 5000 cells, the system was propagated for 1250 steps. To avoid effects from the cell borders, all quantities were calculated only for the central 2500 cells (L = 2500). The choice of L is mainly based on computational resources available. We tested L = 5000 to be able to perform approximately 500 ensemble members. For a selected rule, rule 20 (see below for more details), we performed a test with L = 20000 but the number of members was limited to 10 for the limits in computational resources. We would like to stress that this test, as well as the scaling tests reported in the Results section show that the considered sizes are enough to reach convergence and support our conclusions. For a representative subset of rules, we have run more realizations to investigate the statistics of the rule and its sensitivity to the initial conditions. Most rules behave unspectacularly in this respect. For the interesting cases reported in the main text, 512 runs with different random seeds were performed. Critical β exponents were calculated over the first 50 temporal iterations for all the 512 simulations. Mean values of β parameters and corresponding standard deviations are reported in the section below.

The main considered quantity is the surface width, W, and its dependence on length and time. W is defined as

$$W(L,t) = \langle \frac{1}{L} \int_0^L (h(x,t) - \overline{h}(t))^2 dx \rangle^{1/2} \tag{1}$$

To identify the universality class of a rule, the Family-Vicsek scaling relation [17] was employed:

$$W(L,t) \sim L^{\alpha} f(\frac{t}{L^z}) \tag{2}$$

where f is a function such that $f(u) \propto u^{\beta}$ for $u \ll 1$ and $f \propto$ constant for $u \gg 1$, t is the time, and L the length. α, β, and $z = \alpha/\beta$ are the critical exponents, and models with the same critical exponents belong to the same universality class. In a model following the Family-Vicsek scaling relation, W first grows with time as t^{β}, then it saturates. At large times, $W \propto L^{\alpha}$.

3. Results

In Fig. 3, we show the results of the dynamics for two representative rules, namely the rules 4 and 36. Rule 4 fills an empty cell if it has 3 filled neighbouring cells, rule 36 fills an empty cell if it has either 3 or 6 filled neighbouring cells. The surface is shown as a continuous line after 50 iterations (green), 500 iterations (yellow), and 1250 iterations (cyan). The cells that are filled after 2500 iterations are shown as black spots in the graph. The evident difference in 'smoothness' of the surface, which can be seen with naked eye, can be made quantitative by the analysis of the surface width and its behaviour: rule 4 does not display any saturation of the surface width W, which continues to grow indefinitely, while for rule 36 the width saturates to a finite value. Even though W continues to grow indefinitely in rule 4, still the roughness exponent converges to a finite value. Similar considerations were made for all the rules.

The 256 non-trivial outer-totalistic pure-growth rules in (1+1) dimensions considered here can be classified in 3 main classes, according to the observed growth behaviour: (a) rules showing a saturating behaviour; (b) rules with indefinite growth of the surface width W; (c) non-growing rules. Roughness exponent α and the growth exponent β for 32 representative rules from classes a and b are shown in Fig. 4, together with the most representative models of surface growth. As shown in Fig. 4, the rules clearly group in clusters: the rules belonging to the same cluster have very similar exponents, clearly separated from the other clusters in the α-β plane. The clusters represent a finer structure of classification with respect to the classification in classes. Some rules have the same exponents for obvious reasons (for example, they differ only by their behaviour when all 8 neighbours are full), in other cases the equivalence of behaviour could have not been foreseen without explicitly simulating the rule dynamics. Before discussing more in detail the results shown in Fig. 4, we proceed to comment on the different classes separately.

3.1. Saturating class

The rules belonging to this class display a long-term saturation of the surface width: there is initially a transient, non-universal behaviour, followed by a regime where the surface width $W \propto t^{\beta}$, and finally by saturation to a limiting value, characterized by the roughness exponent

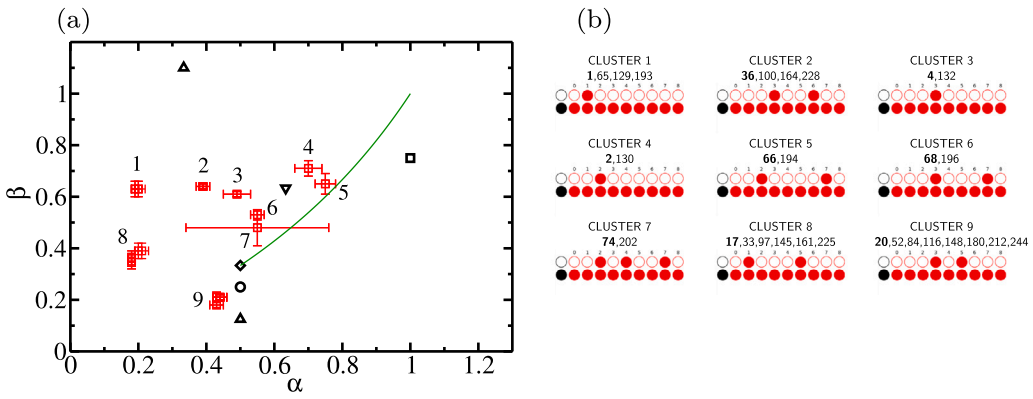

Fig. 4. (a) Critical exponents of the surface growth of (1+1) cellular automata (CA), together with the critical exponents of some known models. α is the roughness exponent; β is the growth exponent. Red squares: critical exponents from 512 realizations of each CA. The bars represent the standard deviations of α and β. Each cluster is marked with a number labelling rules with similar behaviour. Clusters 1, 2, 6, 8 and 9 belong to the saturating class, while the clusters 3, 4, 5, 7 belong to the dendritic-growth class. The rules composing each of the nine clusters are detailed in the SI. Black circle: Edward-Wilkinson model; black square: quenched Edward-Wilkinson model; black rhombus: Kardar-Parisi-Zhang model; black triangle down: quenched Kardar-Parisi-Zhang model; solid dark green line: models with correlated noise from Ref. [16]; black triangles up: other continuum classes (see SI). (b) Composition of each cluster with the corresponding rules numbers. The rule numbers in bold is represented with a schematic of the rule function, for example Cluster 1 is composed by rules 1, 65, 129, 193 and rule 1 is displayed. The full representation of all rules grouped by clusters is reported in the SI. (For interpretation of the references to colour in this figure legend, the reader is referred to the web version of this article.)

α, $W \propto L^{\alpha}$, where L is the size of the system. Clusters 1, 2, 6, 8, and 9 belong to this class. Moreover, cluster 9 has the more stringent feature of displaying dynamic Family-Vicsek (F-V) scaling: the dynamic F-V scaling of W appears when, normalizing the ordinate and the abscissa by L^{α} and L^{z}, all W curves for different L collapse to a single one, as shown in Fig. 5. The appearance of Family-Vicsek (F-V) scaling is the first unexpected result of this work: F-V scaling was originally derived for continuum models with stochastic dynamics, while here discrete models with a deterministic dynamics are considered. The other clusters do not provide evidence of a clear collapse of scaled growth curves , see SI where we show the scaling plot for a representative rule for each cluster. In particular cluster 1 shows a collapse for short characteristic lengths, up to L = 625, while for L = 1250, 2500 there is an underestimation of the scaled W at saturation. Cluster 2, 6 and 8 do not show collapsing curves at all. Clusters have different exponents from one another, i.e. they represent different universality classes. Cluster 9 is closest to Edward-Wilkinson and Kardar-Parisi-Zhang universality classes in the α-β plane, but the analysis of the exponents extracted from several starting seeds suggests that the difference is statistically significant (see SI). The other clusters lie far from any known universality class.

For each cluster, the fractal dimension can be calculated from the roughness exponent α as $d_f = 2 - \alpha$ [21], giving $d_f = 1.81, 1.62, 1.47, 1.82$ and 1.57 for the clusters 1, 2, 6, 8, and 9, respectively.

3.2. Dendritic-growth class

A second class of rules offers an intriguing behaviour: the rules do not follow the saturating behaviour of the first class because the surface width W continues to grow indefinitely, following a behaviour observed only in non-linear differential equations for dendritic growth. However, even in these cases, W still initially grows as t^{β}, and the roughness exponent converges to a finite value with time, so that a well defined α can be calculated and well describes the limiting behaviour of the rule at long times. Also rules from this class are therefore reported in Fig. 4. As for the saturating class, also the rules from the dendritic-growth class clearly group in clusters: clusters 3, 4, 5, and 7 belong to this class. By inspection of the CA configurations during the simulations, the reason for the peculiar behaviour of this class has been identified in the presence of 'pits', i.e. of local configurations on the surface that do not grow at all, and are invariant under the rule dynamics. This ensures that they continue to exist indefinitely, and that remain at the same height (or depth), while the rest of the surface keeps growing. The formation of these pits depends on the rule, and they have a finite density on the surface. Their contribution dominates W, and the result is that W diverges with time. A simple model of surface growth with non-growing pits shows that W will be linear in the height of the growing part of the surface, i.e. W will be dominated by the height difference between the advancing front and the (static) bottom of the pits (see the SI).

Also in this class, most of the clusters of rules are far from any known universality class. Cluster 7 is close to the line given by a family of models for spatially correlated ballistic deposition from Ref. [16]. In any case, since these CA do not obey Family-Vicsek scaling, their behaviour had to be regarded as fundamentally different even if the exponents coincided.

The clusters 3, 4, 5, and 7 have fractal dimensions of 1.52, 1.31, 1.28, and 1.34, respectively. The fractal dimensions of the surfaces from the dendritic-growth class are lower than those from the Family-Vicsek class, as the corresponding roughness exponents α are higher.

3.3. Non-growing class

Class *c* contains the rules where growth stops after few steps, or does not take place at all. This is because the growth conditions are never realized at the surface (for example, the rule where the cell gets filled only if it has 8 full neighbours). These cases are trivial and have not been analysed further (see SI).

3.4. Connection between rule and exponents

The analysis of the rules in terms of critical exponents identifies nine clusters of rules, belonging either to class *a* or class *b*. Within each cluster, the rules behave in a very similar way. Here we analyse the connection between the rule (i.e. which numbers of filled neighbours activate growth) and the behaviour of the CA in terms of critical exponents. The clusters 1-6 show β higher then 0.5 and large variability in terms of α. Clusters 1 to 6 are characterized by growing when only one surrounding site occupation level is met in the range 1-3. For example, cluster 1 contains the rule 1 that activates growth when only one surrounding site is occupied. Moreover, the differences among clusters 1-6 are controlled by response to occupation levels 6-7. The remaining clusters, 7-9, show lower β with variable α. Cluster 7 activates growth when 2, 4, 7 surrounding sites are filled. Rules generating cluster 8 are similar to the ones in cluster 1 but involve also occupation levels 5 or 6. Cluster 9 is composed by all the rules that grow with 3 or 5 occupation levels and any configuration for occupation higher than 5.

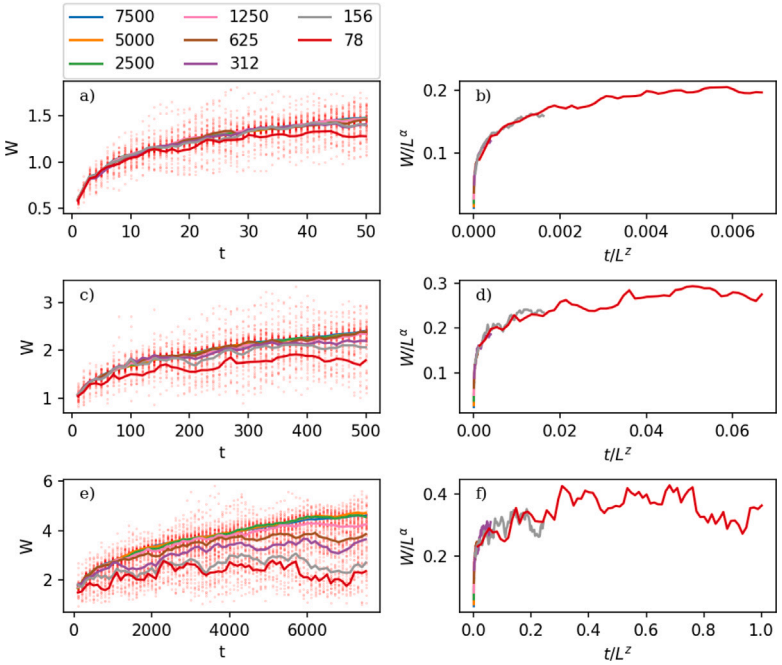

Fig. 5. Family-Vicsek scaling over the average of ten randomly initialized realizations of rule 20 (cluster 9) on a domain of size 20000. Time evolution of the surface roughness W for 8 different characteristic lengths (L = 78, 156, 312, 625, 1250, 2500, 5000, 7500) shown with different temporal sampling: every step (panel a) every 10 steps panel (c) and every 100 steps (panel e). Normalized plots sampling every step (panel b) every 10 steps panel (d) and every 100 steps (panel f) are reported. The corresponding parameters are growth exponent $\beta = 0.21 \pm 0.02$, roughness exponent $\alpha = 0.43 \pm 0.01$ and dynamic exponent z = 2.04. Red scatter dots are the W from simulation members before averaging.

It has to be noticed that clusters from the saturating class (clusters 1, 2, 6, 8, 9) tend to have a smaller α with respect to the clusters from the dendritic-growth class (clusters 3, 4, 5, and 7). Still, clusters from the two classes can be quite close in the plane: cluster 2 is closer to cluster 3 than to any other cluster. Cluster 9 and 7 are quite close to theoretical models obeying the Family-Vicsek scaling.

3.5. Bifurcations

As described in the Methods section, for the interesting rules we ran 512 realizations to investigate the statistics of the rule and its sensitivity to the initial conditions. While most rules behave unspectacularly in this respect, a noticeable behaviour is seen in the rules in cluster 2 and 7. There, as shown in Fig. 6, a bifurcation behaviour is observed for W as a function of time. Some realizations fall into the long-term steady state from the start, while others follow a high-W branch. The two clusters belong to different classes: cluster 2 belongs to the saturating class, while cluster 7 belongs to the dendritic-growth class. This is reflected in the long-term fate of the branching: in cluster 2, the realizations that follow the high-W branch(es) tend to decay into the low-W steady state, so that at long times the low-W prevails. This is reflected in the fact that the standard deviation of α is low for cluster 2, but it is huge for cluster 7 (see Supporting Information). Indeed, in cluster 7 the branching is permanent, i.e. it exists also in the steady state. In cluster 7 this behaviour is related to the emergence of singular structures, triggered by specific combinations of the initial conditions, that are conserved with time. Still, even in this case, the variability of the dynamic exponent of a rule is limited, to the point that the dynamic exponents of different rules are different from one another at a statistically significant level.

4. Discussion

The present work offers insight on two issues: the classification of cellular automata, and the capabilities of cellular automata as models of growth. Regarding classification, the investigation of growth behaviour provides an elegant, flexible, and quantitative way to classify the CAs considered here: it clearly distinguishes three main classes: the saturating class, the dendritic-growth class, and the non-growing class. As suggested also by Fig. 3 and by the Supporting Information, the difference in behaviour among the three classes is striking to the point that visual inspection of the growing interface already gives a clear idea about the class the rule belongs to. Then, quantitative analysis providing the roughness exponent and the growth exponent of each rule makes it possible to identify the fine structure of the classification, with each of the two first classes displaying a further division in clusters, as shown in Fig. 4. This classification is quite robust as the differences in exponents among the clusters are considerably larger than statistical errors and fluctuations arising from the random nature of the initial seed or the numerical analysis to extract the exponents. Moreover, we argue that a similar analysis could be performed also on other cellular automata beside those of pure growth considered in this work; therefore, this classification has the potential to become a universal tool for classification of cellular automata, also for other dimensions. This goes however beyond the scope of the present work.

At the same time, the exponents also provide a picture on how clusters of cellular automata describe growth regimes that are completely different from one another, in the sense that they represent distinct universality classes of growth. The search for novel universality classes is an active field of research, specially in non-equilibrium physics [22], and for this reason it is interesting to discuss the relation between the present CAs and existing theoretical models and experimental systems, for which critical exponents have been determined.

The main models for surface growth in (1+1) dimensions are reported in the $\alpha - \beta$ plane in Fig. 4. Some of the CAs considered here appear also to be close to known models of growth. Cluster 9 from the saturating class lies close to the Edward-Wilkinson model ($\alpha = 0.5$ and $\beta = 0.25$), but the difference appears to be statistically significative (see Supporting Information). Beside this, also the universality class comprising the quenched KPZ [23] and the directed percolation depinning model [24–26] ($\alpha \sim 0.633$ and $\beta \sim 0.633$ [23]) is relatively near to some of our CAs, but also in this case the difference is statistically significative (see Supporting Information). Finally, our cluster 7 (of the dendritic-growth class) falls on the α-β line drawn by the models with

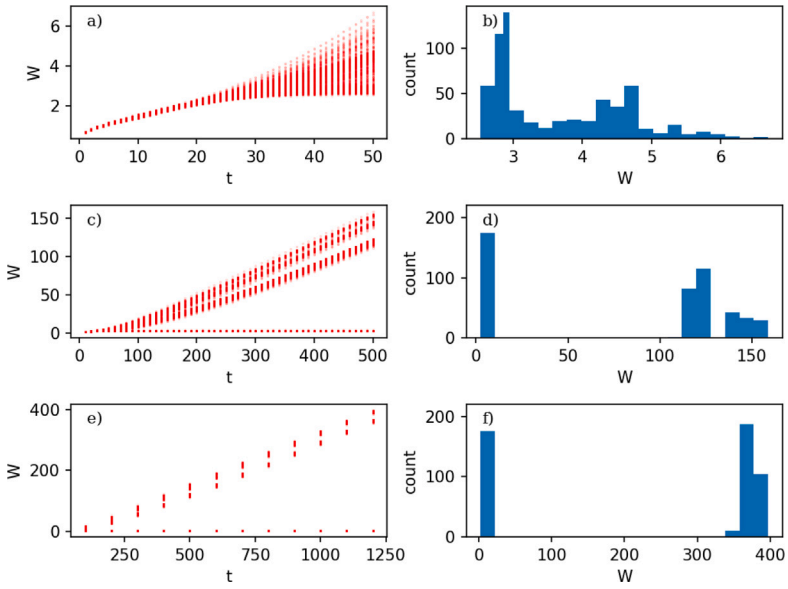

Fig. 6. Evolution of W for the rule 74, for 512 different realizations of the seed, plotted with different temporal sampling: every step (panel a) every 10 steps (panel c) and every 100 steps (panel e). The W histograms at 50, 500, 1250 iterations are shown in panels (b), (d), (f) respectively. The branches of low W and high W are clearly visible. This rule belongs to the cluster 7, of the dendritic-growth class.

correlated noise from Ref. [16] (Fig. 4). In this respect, it should be also noted that, apart from cluster 9, the clusters that appear close to, but distinct from, these known universality classes all belong to the dendritic-growth class and not to the saturating class like the theoretical models mentioned above, which reinforces the idea that, while lying near in the $\alpha - \beta$ plane, they truly represent fundamentally separate classes.

Experimentally, the (1+1) dimensions employed in the current work correspond to a number of experimental situations, like domain growth in nematic liquid crystals [27,28], the growth of domains in magnetic thin films, like those relevant for magnetic memories in recording technologies [29–33], and paper burning [34,35]. Depending on the nature of the interfaces and external driving provided, interfaces growing in nematic liquid crystals was experimentally shown either to belong to the KPZ universality class in (1+1) dimensions [27], or to display $\alpha \sim 0.4$ and $\beta \sim 0.2$ [28], in agreement with the Allen-Cahn (Model A) class; this lies interestingly close to some of our cellular automata (see Fig. 4), namely to our cluster 9 (of the saturating class). Also in this case, the differences are statistically significative. In magnetic domain walls in thin films, several experiments found values of $\alpha = 0.66$-0.81 [29–33]. Varying temperature and applied electric field, Rapin et al. found a wider range $\alpha = 0.5$-0.8 [22], and a dynamic exponent $z = 0.21$. The burning and the flame fronts in paper burning belong to the KPZ universality class in the slow-burning regime [34], but the burn front display $\alpha = 0.88$ at small scale and high burning speed [35].

In continuous linear models, such as E-W, scaling can be derived by simple operations on the corresponding partial differential equations. Even for the non linear models (e.g. KPZ in 1D) renormalization techniques can be used to derive the scaling exponents. In the present case among the 32 selected rules it seems difficult to predict by analytic means α and β according to the specific features of the rule. Moreover the deterministic nature of CA has a particular effect: singular structures generated for specific combinations of the random seed can induce complex unexpected behaviour [36] as in the present case for rule 74 where bifurcations on W roughness are observed. Similar behaviour seems difficult to reproduce with continuous models. The lack of noise in the dynamics preserves the singular structures of deterministic discrete rules.

5. Conclusion

Cellular automata are simple deterministic discrete rules that can lead to a wide range of behaviours, from simple to very complex, and it would therefore be useful to have a criterion to classify them on the basis of their behaviour. Here, we have considered cellular automata of pure growth and analysed surface growth in (1+1) dimensions as described by their dynamics. With respect to surface growth, the cellular automata can be classified in three classes: the saturating class of CAs, characterized by saturation after initial growth (which includes also rules obeying the dynamic Family-Vicsek scaling), the dendritic-growth class of CAs displaying indefinite growth of the surface width, and the non-growing class. For each of the first two classes, consideration of the critical exponents α (roughness exponent) and β (growth exponent) lead to a sub-division in clusters. This fine structure is immediately visible in the graphical representation of the classes in the α-β plane. We argue that this classification criterion is quantitative and robust, and could therefore be useful also beyond the family of cellular automata considered in the present work.

Moreover, this work shows that cellular automata are an attractive tool to reproduce natural phenomena that display a comparable wealth of regimes. One such phenomenon is growth, which is ubiquitous, being present in systems from plankton colonies, through living cells, tumours, cities, to materials, surfaces, and nanoparticles, and which have regimes from regular to dendritic. In the α-β plane, some of the rules are near to known universality classes, such as those of the Edward-Wilkinson and the quenched Kardar-Parisi-Zhang models, or to experimental data, e.g. for domain growth in magnetic thin films, while others fall in regions where no other data exist.

This underlines the richness of the phenomenology produced by the deterministic cellular automata, their potential for the study of growth phenomena, and their growth behaviour as a possible tool for their classification.

Code availability

The code and analysis tools used for the current study are available in the REPORT 1+1 repository https://doi.org/10.5281/zenodo.6990025.

CRediT authorship contribution statement

Paolo Lazzari: Writing – review & editing, Writing – original draft, Visualization, Software, Formal analysis, Conceptualization. **Nicola Seriani:** Writing – review & editing, Writing – original draft, Methodology, Formal analysis, Conceptualization.

Declaration of competing interest

The authors declare that they have no known competing financial interests or personal relationships that could have appeared to influence the work reported in this paper.

Data availability

The code for generating the data is available on Zenodo, see section Code availability.

Appendix A. Supplementary data

Supplementary material related to this article can be found online at https://doi.org/10.1016/j.chaos.2024.114997.

References

[1] Von Neumann J, Burks AW. Theory of self-reproducing automata. Urbana, Illinois, U.S.A.: University of Illinois Press; 1966.
[2] Gardner M. The fantastic combinations of John Conway's new solitaire game "life". Sci Am 1970;223:120–3.
[3] Manukyan L, Montandon SA, Fofonjka A, Smirnov S, Milinkovitsch MC. A living mesoscopic cellular automaton made of skin scales. Nature 2017;544:173–9.
[4] Edelstein-Keshet L. How the lizard gets its speckled scales. Nature 2017;544:170.
[5] Wootton JT. Local interactions predict large-scale pattern in empirically derived cellular automata. Nature 2001;413:841–4.
[6] Kansal AR, Torquato S, Harsh GR, Chiocca EA, Deisboeck TS. Simulated brain tumor growth dynamics using a three-dimensional cellular automaton. J Theoret Biol 2000;203:367–82.
[7] Rendell P. Game of life universal turing machine. In: Turing Machine Universality of the Game of Life, vol. 18, Springer International Publishing; 2016, p. 192. http://dx.doi.org/10.1007/978-3-319-19842-2_5, Series Title: Emergence, Complexity and Computation. URL http://link.springer.com/10.1007/978-3-319-19842-2_5.
[8] Wolfram S. A new kind of science. Champaign, Illinois, U.S.A.: Imprint Wolfram Media; 2002.
[9] Vispoel M, Daly AJ, Baetens JM. Progress, gaps and obstacles in the classification of cellular automata. Phys D 2022;432:133074.
[10] de Sales JA, Martins ML, Moreira JG. One-dimensional cellular automata characterization by the roughness exponent. Phys A 1997;245:461.
[11] Takeuchi KA, Sano M, Sasamoto T, Spohn H. Growing interfaces uncover universal fluctuations behind scale invariance. Sci Rep 2011;1:34.
[12] Orrillo PA, Santalla SN, Cuerno R, Vasquez L, Ribotta SB, Gassa LM, Mompean FJ, Salvarezza RC, Vela ME. Morphological stabilization and KPZ scaling by electrochemically induced co-deposition of nanostructured NiW alloy films. Sci Rep 2017;7:17997.
[13] Personick ML, Mirkin CA. Making sense of the mayhem behind shape control in the synthesis of gold nanoparticles. J Am Chem Soc 2013;135:18238–47.
[14] Kardar M, Parisi G, Zhang Y-C. Dynamic scaling of growing interfaces. Phys Rev Lett 1986;56:889–92.
[15] Edwards SF, Wilkinson DR. The surface statistics of a granular aggregate. Proc R Soc Lond Ser A Math Phys Eng Sci 1982;381:17.
[16] Meakin P, Jullien R. Spatially correlated ballistic deposition on one- and two-dimensional surfaces. Phys Rev A 1990;41:983.
[17] Family F, Vicsek T. Scaling of the active zone in the Eden process on percolation networks and the ballistic deposition model. J Phys A: Math Gen 1985;18:L75–81. http://dx.doi.org/10.1088/0305-4470/18/2/005.
[18] Sasamoto T, Spohn H. The 1 + 1-dimensional Kardar–Parisi–Zhang equation and its universality class. J Stat Mech 2010;P11013. http://dx.doi.org/10.1088/1742-5468/2010/11/P11013.
[19] Masoudi AA, Shahbazi F, Davoudi J, Rahimi Tabar MR. Statistical theory for the Kardar-Parisi-Zhang equation in (1+1) dimensions. Phys Rev E 2002;65:026132. http://dx.doi.org/10.1103/PhysRevE.65.026132.
[20] Spohn H. The 1+1 dimensional Kardar–Parisi–Zhang equation: more surprises. J Stat Mech 2020;044001. http://dx.doi.org/10.1088/1742-5468/ab712a.
[21] Barabasi AL, Stanley HE. Fractal Concepts in Surface Growth. Cambridge, U.K.: Cambridge University Press; 1995.
[22] Rapin G, Ehrensperger S, Blaser C, Caballero N, Paruch P. Dynamic response and roughening of ferroelectric domain walls driven at planar electrode edges. Appl Phys Lett 2021;119:242903.
[23] Santalla SN, Ferreira SC. Eden model with nonlocal growth rules and kinetic roughening in biological systems. Phys Rev E 2018;98:022405.
[24] Buldyrev SV, Havlin S, Stanley HE. Anisotropic percolation and the d-dimensional surface roughening problem. Phys A 1993;200:200.
[25] Leschhorn H. Anisotropic interface depinning: Numerical results. Phys Rev E 1996;54:1313.
[26] Odor G. Universality classes in nonequilibrium lattice systems. Rev Mod Phys 2004;76:663.
[27] Takeuchi KA, Sano M. Universal fluctuations of growing interfaces: Evidence in turbulent liquid crystals. Phys Rev Lett 2010;104:230601.
[28] Almeida RAL, Takeuchi KA. Phase-ordering kinetics in the Allen-Cahn (Model A) class: universal aspects elucidated by electrically-induced transition in liquid crystals. Phys Rev E 2021;104:054103.
[29] Jordan D, Albornoz LJ, Gorchon J, Lambert CH, Salahuddin S, Bokor J, et al. Statistically meaningful measure of domain-wall roughness in magnetic thin films. Phys Rev B 2020;101:184431.
[30] Ziegler B, Martens K, Giamarchi T, Paruch P. Domain wall roughness in stripe phase BiFeO3 thin films. Phys Rev Lett 2013;111:247604.
[31] Cortes Burgos MJ, Guruciaga PC, Jordan D, Quinteros CP, Agoritsas E, Curiale J, et al. Field-dependent roughness of moving domain walls in a Pt/Co/Pt magnetic thin film. Phys Rev B 2021;104:144202.
[32] Albornoz LJ, Guruciaga PC, Jeudy V, Curiale J, Bustingorry S. Domain-wall roughness in GdFeCo thin films: Crossover length scales and roughness exponents. Phys Rev B 2021;104:024203.
[33] Lee K-S, Lee C-W, Cho Y-J, Seo S, Kim D-H, Choe SB. Roughness exponent of domain interface in CoFe/Pt multilayer films. IEEE Trans Magn 2009;45:2548.
[34] Maunuksela J, Myllys M, Kahkonen OP, Timonen J, Provatas N, Alava MJ, et al. Kinetic roughening in slow combustion of paper. Phys Rev Lett 1997;79:1515.
[35] Balankin AS, Matamoros DM. Anomalous roughness with system-size-dependent local roughness exponent. Phys Rev E 2005;71:056102.
[36] Gray L. A mathematician looks at Wolfram's new kind of science. In: Notices of the American mathematical society, vol. 50, (no. 2):Citeseer; 2003, p. 200–11, URL http://www.ams.org/notices/200302/fea-gray.pdf.